Serviceability Criteria for LRFD Composite Floors

Roberto T. Leon

Author

Roberto T. Leon is associate professor in the Department of Civil and Mineral Engineering at the University of Minnesota. He teaches courses in structural steel design, construction materials, and earthquake engineering. He received a bachelor of science in civil engineering from the University of Massachusetts at Amherst, a master of science in structural engineering from Stanford University, and a Ph.D. from the University of Texas, at Austin. He is a registered professional engineer in Minnesota and is active on technical committees of the American Institute of Steel Construction, American Society of Civil Engineers, Structural Stability Research Council and the American Concrete Institute.

Dr Leon's research interests center on behavior of semi-rigid connections, behavior of composite joists, bridge rating and rehabilitation, and serviceability criteria for composite members. He has conducted extensive experimental research on composite and reinforced concrete members and connections under static and dynamic loads, as well as field tests on bridges, buildings and illumination towers.

Summary

The trend toward limit state design codes for steel and composite structures has resulted on an emphasis of strength requirements over serviceability requirements, particularly for codes issued in the United States. As a result, the *Load and Resistance Factor Design Specification* (LRFD), can produce substantial economics in materials (10% to 15%) for LRFD-designed composite beams over ASD-designed ones. Many of the savings, however, come from utilizing very shallow sections over long spans. This raises some questions as to potential serviceability problems since the LRFD Specification contains no specific serviceability criteria.

This paper addresses serviceability issues, primarily short and long-term deflections for composite beam floors designed to American specifications. It describes the results of tests conducted to determine the effects of (1) cambering and shoring, (2) creep and shrinkage, and (3) end restraint on deflections of slender composite girders. It discusses the pertinent limit states, and offers recommendations and guidance on how to calculate deflections for composite floors.

SERVICEABILITY CRITERIA FOR LRFD COMPOSITE FLOORS

INTRODUCTION

Composite floor systems have long been recognized as the most economical system for multi-story buildings. Whether consisting of composite joists, composite trusses or composite beams, their ease of construction and strength/weight ratio make them the system of choice, particularly in tall tube-within-tube or similar structures [1,2]. For these types of floor systems, the Load and Resistance Factor Design Specifications (LRFD) [3] can produce substantial economies in materials (10% to 15%) for LRFD-designed composite beams over ASD-designed ones [4]. Many of the savings, however, come from utilizing very shallow sections over long spans. This raises some questions as to potential serviceability problems since the LRFD Specification contains no specific serviceability criteria.

This paper addresses serviceability issues, primarily short and long-term deflections, for composite beam floors designed to American specifications. It discusses the pertinent limit states and offers recommendations and guidance on how to calculate deflections for composite floors. It also describes the results of tests conducted to determine the effects of (1) cambering and shoring, (2) creep and shrinkage, and (3) end restraint on deflections of slender composite girders.

LIMIT STATES DESIGN

The LRFD Specification is based on a limit state design philosophy, in which prescribed limit states should not be exceeded. A limit state can be broadly defined as a limit of structural usefulness, and can be categorized into two general groups: ultimate strength criteria and serviceability criteria. Ultimate strength criteria are usually associated with preventing brittle failure or collapse and safeguarding human life. Serviceability criteria, on the other hand, aim at preventing occupant discomfort (whether real or perceived) and the associated economic losses to the owner. Some common serviceability criteria intend to prevent excessive deflections or vibrations, and unsightly cracking or similar damage to the non-structural elements of the building.

Most engineers have no trouble at all with these concepts at the qualitative level, but would like to have some additional quantitative guidance from a specification. In other words, no engineer likes his floors to deflect excessively, but what is excessive? The LRFD Specification, by choice, offers no such guidance. For example, insofar as deflections is concerned, it states that "deformations in structural members and structural systems due to service loads shall not impair the serviceability of the structure." The discussion in the Commentary is only slightly less vague, stating that "such limits would depend on the use of the structure." In the absence of such values, most engineers in the U.S. will assume either the old deflection limit of L/360 or span/depth ratios such as $F_y/1000$ or $F_y/800$ as their limits. Other limit state codes are only marginally better in this area. For example the Canadian Specification [5], while giving some detailed values in an appendix for simply-supported beams, does not offer much guidance for continuous floor systems.

It is interesting to note that traditional criteria such as L/360 have served well for many years, and probably need not be changed. In general when serviceability problems arise it is because the deflections were not calculated correctly. Assuming that human error is not involved, the most likely source of error is the model used to calculate the deformations. It is the author's contention that our current models for calculating deflections of composite floors are inadequate, and are responsible for many of the serviceability problems found in the field. Four key areas where current models are inadequate are (1) the calculation of stresses after the construction loads have been applied, (2) the calculation of the moment of inertia to be used, (3) the long-term effects of creep and shrinkage, and (4) the effect of continuity and end restraint.

In this context it is important to highlight the fact that limit states design theory considers the violation of a modelling assumption to be a violation of a limit state. In the particular case of composite beams, for example, this means that calculating service load deflections using elastic theory is valid only insofar as the system remains elastic. This may seem like a statement of the obvious, but in the LRFD Specification there *is* no check to insure that the beam has remained elastic under the service live loads. In the following sections modelling shortcomings will be discussed in some detail. These theoretical considerations will then be illustrated with the results of some experimental data generated recently.

INITIAL STRESSES

The ASD Specification contained an equation (Eq. (1.11-2)) which effectively assured elastic behavior at service loads for most design situations in unshored construction. This equation:

$$S_{tr} = (1.35 + 0.35(M_L/M_D)) S_s \qquad \text{Eq. [1]}$$

where S_{tr} was the transformed moment of inertia, M_L was the live load moment, M_D was the dead load moment, and S_s was the moment of inertia of the beam alone, effectively limited the section modulus to be used in calculating dead load stresses if the dead load moment was high. As pointed out before, no similar check is required in LRFD. This is an important point because under the LRFD provisions the selection of a steel section to be used in a composite floor will generally be governed by construction loads. Thus the steel beam maybe stressed near yield before the live loads are applied.

To ensure that elastic analysis is applicable to unshored construction, the stress due to the service live load (f_{LL}) must be less than the difference between the actual steel yield stress (f_y) and the dead load stresses (f_{DL}) due to the weight of the concrete and other loads applied before the concrete hardened, the stresses due to cambering (f_C), and any residual stresses (f_{RS}) present after rolling of the beam. This can be written as:

$$f_{LL} < f_y - [f_{DL} + f_C + f_{RS}] \qquad \text{Eq. [2]}$$

In general it is safe and conservative to assume the nominal F_y as f_y as the material supplied will almost always exceed its nominal yield strength. The calculation of f_{DL} is not as simple, since it implies an accurate knowledge of

all dead loads, including partitions and permanent equipment. From the practical standpoint f_C is unknown, and only very rough estimates can be made for f_{RS}

Figure 1 shows a typical residual stress distribution in an I-beam after rolling (Fig. 1a), after straightening (Fig. 1b), the stresses due to cold cambering (Fig. 1c), and a possible final stress distribution just before the beam is placed into position (Fig 1d). The figure shows that parts of the beam will be at up to 50% of yield, and that if a uniform bending stress is applied, some parts of the beam will yield much sooner than others. The residual stress distribution has no effect on the ultimate strength of the beam, but can have a significant effect on the limit of linear elastic behavior. As soon as yield starts in the section, the moment of inertia will decrease and so will the stiffness of the floor system.

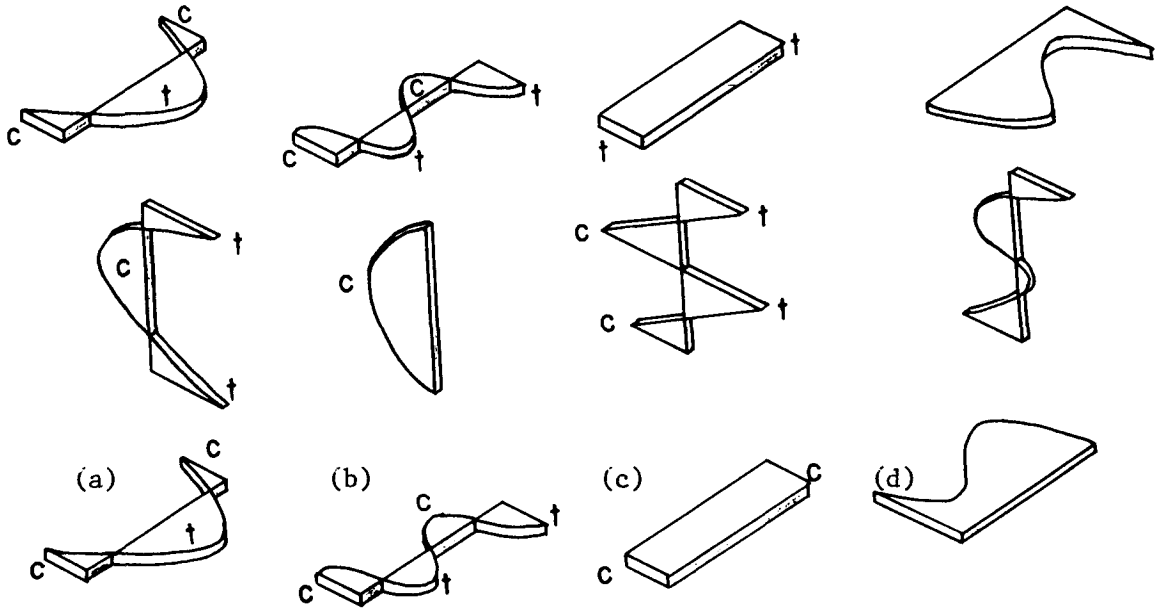

Figure 1 - Residual stress distributions in I-beams.

For the case of shored construction cambering stresses do not exist, and the stresses in the beam before the shores are removed f_{SH} must be substituted for f_C in Eq. [2]. The shoring stresses f_{SH} can be calculated, and are generally small if a large number of shores is used. Thus an exact calculation of the live load capacity before onset of yielding may be more reliably made for a shored than for an unshored beam. In any case, only an statistical or reliability approach seems reasonable for this problem.

EFFECTIVE MOMENT OF INERTIA

It is well-known that current allowable stress design provisions assume an optimistic value for the effective width of a slab in a composite beam. Comparisons with experimental results show that using elastic moments of inertia based on this methodology underestimate deflections in the service range by 15%

to 25%. Some of the most recent evidence in this area comes from the work of Vallenilla and Bjorhovde [6] and Taylor [7], A typical figure from the latter (Fig. 2) underscores the problem. Typical results using this procedure can be improved by accounting for (1) shear deformations [7], (2) the flexibility of the studs [7], and/or (3) using a different definition for effective width [6]. The former two factors are seldom included in practice, and the latter is only a convenient method to better fit the data.

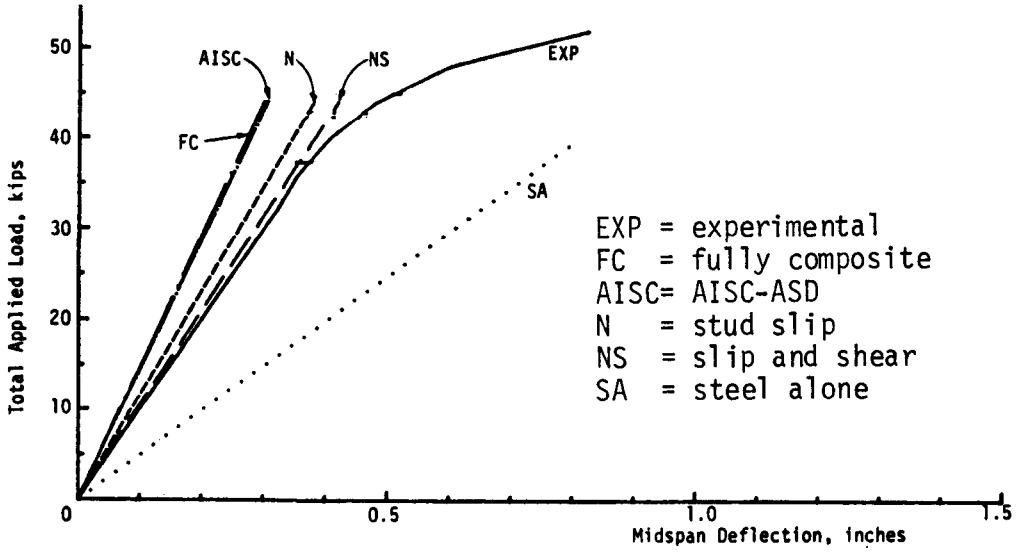

Figure 2 - Comparison of measured and calculated deflections [7].

Some of the work cited above, plus earlier evidence, provided impetus for a much more conservative approach to the calculation of moments of inertia in the new LRFD specifications. The calculations in the LRFD manual are based on an ultimate strength analysis, with a stress block smaller than that assumed in linear elastic transformed section analysis. In general the LRFD procedure limits the size of the concrete flange to the smallest of A_sF_y (total force on the steel section) or to the summation of Q_n (total force on shear studs). While this assumption of equivalent concrete flange is entirely reasonable in ultimate strength calculations, the deflections under service loads will be at significantly lower stress levels. Therefore the use of a "plastic" or lower bound moment of inertia (LBMI) for a computation in the elastic range is theoretically questionable. On the other hand, the procedure typically will result in better correlation with experimental results, since the plastic moment of inertia will be 15% to 30% lower than the elastic one. However, as is the case with the use of alternative effective width definitions, we are no closer by using a LBMI to discovering the behavior mechanisms which will explain the discrepancies between tests and theory.

It should be also noted that most calibrations for effective width have been done on tests carried out with a single point load at the middle rather than with distributed loads. Although the yield and ultimate moment capacity are not very sensitive to the load configuration, the deflections can be significantly affected by the shear distribution along the beam. This is because the slip and shear deformations, which can be used to explain the differences between the measured and calculated deflections [7], are a function of the loading configuration. In particular, a concentrated load tends to impose large local uplift forces on the studs changing the distribution of shear stresses along the

beam. Near the load point almost 80% of the shear stress is carried by the slab, and there is a significant difference on this distribution if the load is applied to the top of the slab or to the bottom beam flange [8].

LONG TERM DEFLECTIONS

One of the most common problems encountered in construction is excessive deflections and cracking of composite floors within 6 to 24 months after the end of construction. The most likely explanation for these problems is the lack of calculation of creep and shrinkage effects on the concrete slab.

Creep and shrinkage of concrete are generally treated together because they share some basic characteristics. First, the dimensional instabilities know as creep and shrinkage arise from the removal of absorbed water from the cement paste, and are partly reversible. Second, most of the factors that influence creep also affect shrinkage, resulting in very similar the strain vs. time curves for both effects. Finally, the magnitude of creep and shrinkage strains in unrestrained concrete specimens is similar (between 600 and 1000 microstrain).

In many cases deflections due to creep and shrinkage can be ignored if certain span-to-depth ratios are adhered to or if rigid continuous construction is used. In continuous reinforced concrete construction creep and shrinkage generally act against one another, have about the same order of magnitude, and their net effect is to cancel each other and to produce small net deflections. In simply-supported composite construction, on the other hand, the effects of creep and shrinkage are generally additive, have the same order of magnitude, and it is therefore unconservative to ignore their contribution when spans are long and/or the beams are shallow.

Shrinkage

When a floor slab is first cast two types of shrinkage, thermal and drying shrinkage, will occur. Thermal shrinkage is associated with the cooling of the member, while drying shrinkage is associated with the moisture loss. For most practical situations in buildings, the thermal shrinkage can be ignored. On the other hand, drying shrinkage can induce appreciable deflections.

Two studies conducted in Canada by Robinson [9] and Brattland and Kennedy [10] indicate that the centerline deflection of typical composite beams and trusses due to drying shrinkage can approach L/1200 to L/1000. Figure 3 shows some of the results by Robinson on a W16x36 with a 5.5 in. slab on 3 in. deck. The specimen had a 30 ft. span and a slab width of 7.5 ft, and used normal-weight concrete. Most of the measured shrinkage took place within the first 40 days after casting and amounted to about L/1200.

The amount of drying shrinkage will depend on the mix proportions, the age of the concrete, the ambient humidity and the geometry of the member. The two most commonly used procedures for estimating drying shrinkage are those proposed by Comite Eurointernationale du Beton (CEB) and the American Concrete Institute (ACI) Committee 209 [11].

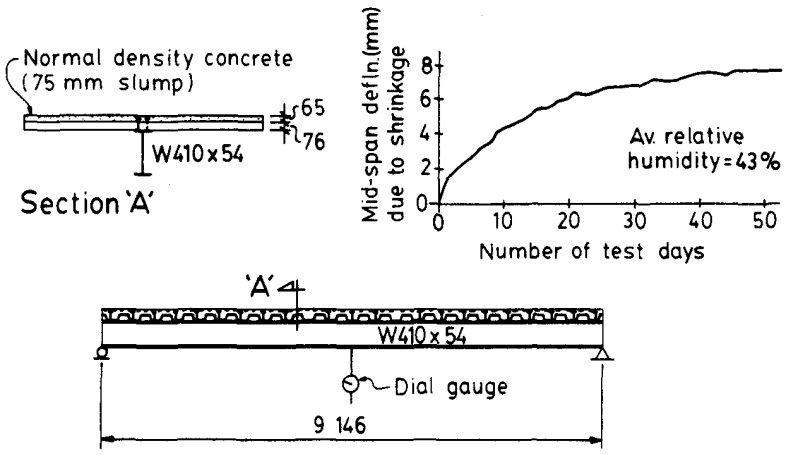

Figure 3 - Shrinkage and creep deflections for a test beam [9].

The ACI equation for unrestrained shrinkage is of the form:

$$\epsilon_{S(t,t0)} = \epsilon_{su} * S_t * S_a * S_h * S_{vs} * S_s * S_f * S_e * S_c$$

where,

ϵ_S = shrinkage strain at time t, from reference time t0
ϵ_{su} = ultimate shrinkage strain
S_t = coefficient for shrinkage from time t0
S_a = coefficient for curing time, if different from 7 days
S_{vs} = coefficient accounting for volume-to-surface ratio
S_h = coefficient accounting for relative humidity
S_s = slump coefficient
S_f = fines coefficient
S_e = air content coefficient
S_c = cement content coefficient

Typical numbers for unrestrained drying shrinkage vary from 600 to 800 microstrain, with ACI suggesting 730 x 10^{-6} in/in if no experimental data is available. When reinforcement is present in a slab or member, the shrinkage is said to be restrained, since the steel reduces the amount of shrinkage that can occur. Recommended values for restrained shrinkage vary from 200 to 400 microstrain. Robinson reported 350 microstrain at 50 days and Kennedy reported 380 and 330 microstrains at 65 days; in both cases these refer to shrinkage of the slab. In Robinson's case this amounted to 2/3 of the shrinkage measured in unrestrained specimens cast along with the composite beam, while in Kennedy's case the restrained shrinkage amounted to about 1/2 of the unrestrained one.

At least one simple method of predicting the amount of deflection due to shrinkage is available. The idea was first presented by Viest [12], and involves replacing the shrinkage strain with a force acting at the centroid of the effective slab as shown in Fig. 4. The procedure requires that this force, acting eccentrically to the neutral axis of the member, be replaced with an equivalent moment applied at the ends of the section. The magnitude of ϵ_{sh} (the drying shrinkage) can be obtained from tests, from the ACI or CEB procedures, or from an informed guess. The ACI and CEB procedures are tedious and require data that is in general unavailable to the designer. A more reasonable approach,

and a long-accepted one, is to assume the shrinkage strain to be 200 microstrain as proposed by Viest [12].

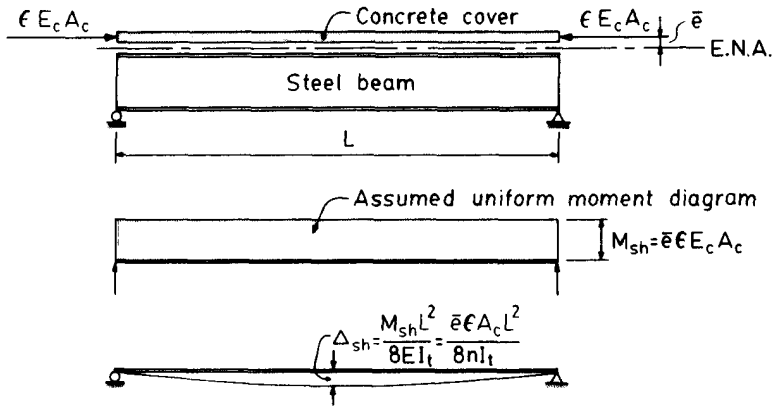

Figure 4 - Calculation of the additional deflection due to shrinkage [12].

Creep

Creep is a stress-relieving mechanism that results in increased shortening of the slab in compression, and will produce additional deflections of the composite beam. Creep is generally important when the ratio of dead load to live load is large or when a large portion of the live load will be present for long periods of time. Current codes do not differentiate between short-term and long-term live loads. While codes do not specify what percentage of the live load should be considered to be long-term, studies have shown that in absence of better information assuming about 25% of full live load to be long-term load is reasonable and conservative.

The typical expression for creep computes the creep strain at time t (ϵ_{ct}) as the product of a creep strain at a reference time t_0, corrected by multipliers to account for ultimate creep, for the time at which creep strain is desired, the age of loading, relative humidity, volume to surface ratio, slump, amount of fines in the concrete mix, and air content. These calculations are valid for concrete under constant stress. ACI 209 suggests an equation as follows:

$$\epsilon_{(t,t0)} = \epsilon_u * k_t * k_a * k_h * k_{vs} * k_s * k_f * k_e * k_c$$

where,

ϵ_s = creep strain at time t, from reference time t0
ϵ_{su} = ultimate creep, taken as 2.35
S_t = coefficient for time at which creep is desired
S_a = coefficient for age of loading
S_{vs} = coefficient accounting for volume-to-surface ratio
S_h = coefficient accounting for relative humidity
S_s = slump coefficient
S_f = fines coefficient
S_e = air content coefficient

S_c = cement content coefficient

Because the concrete will shrink and creep with time, the computed creep strain must be adjusted. A simplified approach to this procedure has been proposed by Bazant [13], who uses the concept of an aging coefficient. The coefficient is used to find an effective modulus of elasticity $(E_{c(eff)})$ for the concrete. This new modulus of elasticity is then used to compute a modified modulus ratio (n), and the creep deflection *is* calculated using elastic analysis formulas and the modified n and E values.

Examples

To illustrate the effects of creep and shrinkage, the long-term deflections for the composite beams used as Examples 1 and 2 in the LRFD Manual will be calculated. The data for both examples are summarized in Table 1. For these cases the deflection due to shrinkage and creep after one year will be calculated following ACI 209 procedures.

Deflections Due to Shrinkage

The ultimate shrinkage (ϵ_{su}) was assumed to be 800 x 10-6, and was modified according to ACI 209 procedures to obtain the actual shrinkage at one year of 537 x 10-6 for Example 1, and 453 x 10-6 for Example 2. These need to be adjusted for the existing restraint and, for the case of Example 1, the lightweight aggregate used. Assuming that the restraint will decrease the shrinkage by one half, and that the lightweight properties will increase shrinkage by 20%, the shrinkage strain after one year will be 322 x 10-6 for Example 1 and 226 x 10-6 for Example 2, resulting in a total deflection of 0.30 in. for Example 1 and 0.46 in. for Example 2.

It should be noted that the computed shrinkage strain is very similar in magnitude to that reported by Canadian researchers. The value obtained, however, is still probably high, and the recommendation by Viest of a shrinkage of 200 microstrain seems more reasonable. Using this value of shrinkage the computed deflection is 0.19 in. for Example 1 and 0.41 in. for Example 2; both of these values appear reasonable since the calculations for shrinkage using ACI 209 could be regarded as an upper bound.

Deflections Due to Creep

The ultimate creep coefficient was assumed to be 2.35, as suggested by ACI 209. Since the modulus of elasticity of the concrete will change with time, an age-adjusted modulus was used in calculating the deflections at 1 year. The age-adjusted modulus can be computed using the tables provided by Bazant [13]. For Example 1, this new ratio (n=15.8) leads to an effective moment of inertia of 1360 in4. For Example 2 the new modulus ratio (n=13.7) leads to an effective moment of inertia of 4748 in4.

Table 1 - Data for Examples 1 and 2 of LRFD Manual

Data	Example 1	Example 2
Construction type	Shored	
Unshored		
Dead load (kips/ft)	0.65	0.90
Live load (kips/ft)	1.00	2.50
Steel strength (ksi)	36	50
Concrete strength (ksi)	3.5	4.0
Concrete density (pcf)	115	145
E for concrete (ksi)	2,408	3,644
Modular ratio (initial)	12.04	7.95
Span (ft)	30	40
Effective slab width (ft.)	7.5	10
Total slab depth (in)	6.25	7.5
Metal deck depth	3.0	3.0
Steel section used	W16 x 31	W24 x 55
Steel area (in2)	9.12	16.2
Tranformed slab area (in2)	24.28	67.93
Elastic neutral axis (in)	5.05	5.53
Elastic moment of inertia (in4)	1,448	5,259
Inelastic moment of inertia (in4)	1,070	4,060
Iinelastic / Ielastic	0.74	0.77
Elastic reduced I (in4)	1,249	4,748

Table 2 - Summary of Deflection Calculations

Component	Example 1	Example 2
Elastic dead load	0.28 (L/1286)	1.33 (L/360)
Shrinkage (1 year)	0.30 (1/1200)	0.46 (L/1043)
Creep (1 year)	0.06 (L/6000)	0.03 (L/8000)
Full LL (1 year)	0.50 (L/720)	1.04 (L/461)
Total deflection	1.14 (L/315)	1.53 (L/313) [*]
Live Load (LRFD Manual)	0.59 (L/610)	1.22 (L/393)

[*] All dead load deflection taken by cambering the beam for Example 2.

The calculation of the contribution of creep to total final deflection is sensitive to the assumptions of which loads are continuously present. In the case of a composite beam built using shored construction arguably all the dead load should be used since once the shores are removed the entire load is transferred to the concrete. Assuming that 25% of the live load was present throughout the first year for both cases, the deflections due to creep are 0.06 in. for Example 1, and 0.03 in. for Example 2.

A very common assumption in order to avoid all the tedious calculations necessary to find an "exact" age-adjusted modulus is to assume that the effective modulus would be the initial modulus divided by 2.5. In this case the calculated deflections for creep increases to 0.10 in for Example 1 and 0.05 in for Example 2. In all cases it seems that creep deflections would not be important provided only a small portion (25%) of the live load is present continuously.

For Example 1 which deals with the design of a shored composite beam, the computed creep and shrinkage deflection of 0.36 in. represents L/1000 (see Table 2). This represents 72% of the deflection under live load (0.50 in) and about 129% of the dead load deflection (0.28 in). The deflection due to shrinkage was about five times greater that due to creep. The superposition of the live load, creep, and shrinkage deflections at one year gives a total deformation of 1.14 in. or L/315. This is almost twice that predicted by the AISC LRFD procedure using a very conservative estimate for moment of inertia. For Example 2 which deals with an unshored composite beam, the computed creep and shrinkage deflection of 0.49 in. represents L/980. This deflection represents 47% of the live load deflection and 37% of the dead load deflections. The deflection due to shrinkage was about 15 times greater than that due to creep. This indicates that we can probably ignore the long and tedious calculations required for creep in unshored construction under most circumstances.

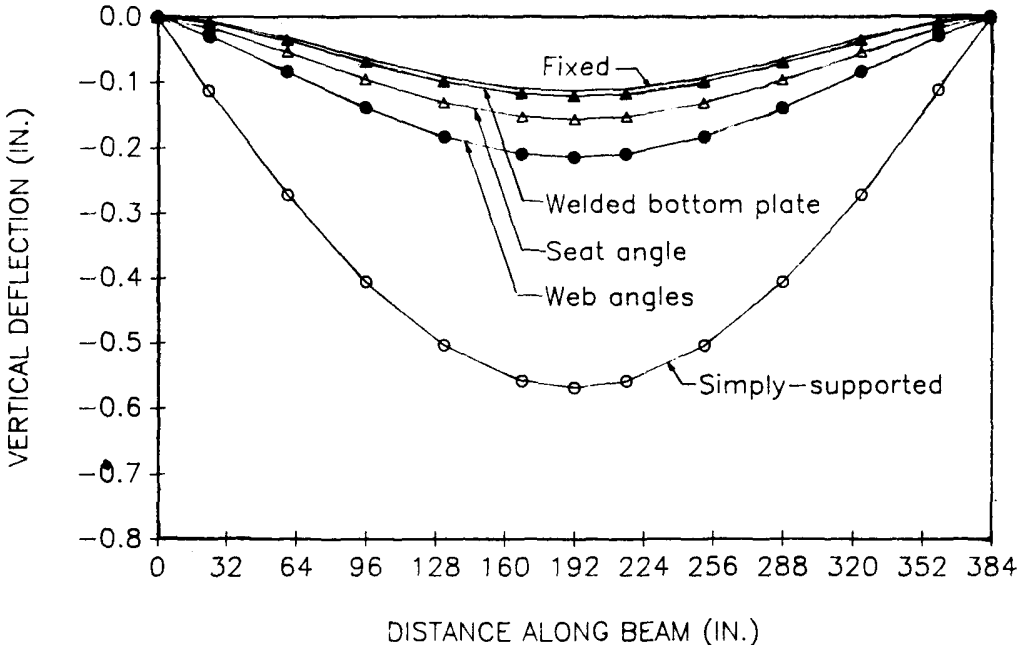

Figure 5 - Effect of end restrain on beam deflections.

EFFECT OF END RESTRAINT

The degree of fixity at the end of a beam can have a significant impact on the total deflection. There is a large amount of continuity in most composite floors, including additional reinforcement over the column lines to decrease the size of cracks. Figure 5 shows the centerline deformations for a composite beam attached to a column given several degrees of semi-rigid end restraint. The beam dimensions for this example are the same as those for the tests described in the next section. For a connection consisting of double web angles and eight #4 rebar in the slab, the reduction in deflection was over 68%. For a connection made up of a large seat angle and the same amount of rebar in the slab, the decrease was close to 72%. Finally, for a connection consisting of a welded bottom plate, web angles, and the same amount of slab rebar, the reduction in deflection was almost 79%. The maximum reduction, of course, is 80%, the ratio of simply-supported to fixed-end deflection. In these calculations experimentally-derived moment-rotation curves were used. The tests also showed the importance of the torquing of bolts in a connection to obtain dependable moment-rotation relationships.

EXPERIMENTAL RESULTS

In order to study the issues discussed above, four long composite girders are currently being tested at the University of Minnesota. The first two beams were tested to determine differences between shored and unshored construction, while the latter two will be used to study the long-term deformations due to creep and shrinkage. The first two tests have been completed, and will be discussed here. While the creep and shrinkage data for these tests refers only to the first sixty days since casting, it is sufficient to demonstrate some of the points made above.

Specimen Description

The composite test specimens consisted of W18x35 beams on 32 ft. spans. The beams were nominally A36 steel, and were all from the same lot in order to minimize the influence of material properties on the final results. The unshored beam specimen (Beam III) was mechanically cambered approximately 3/4 in. to offset deflections due to the concrete self-weight. Strains were monitored in the beam flanges and web during the cambering operations to determine the remaining cambering stresses (f_c). The shored beam (Beam IV) was not cambered. Three shores, spaced at 8 ft., were used to support the beam during casting. The shores used consisted of manual jack with a 25 kip load cell mounted on top, and a wood shim between the load cell and the specimen to distribute the load. The shores were removed five days after casting when the concrete strength exceeded 75% of its specified strength.

The slab was 96 in. wide, cast on 18 gage, 3 in. metal deck. It contained only nominal shrinkage and temperature reinforcement in the form of 6 x 6 x 10/10 welded wire fabric, placed approximately 1 in. from the top of the slab. Ready mix normalweight concrete was used for the floor slabs. The concrete had a nominal 4.0 ksi strength and 3.0 in. slump at the delivery time. Standard compression tests on concrete cylinders taken during the casting process and cured in the same manner as the slab demonstrated average concrete compressive strength of 5.0 ksi at 28 days.

The composite action was achieved with 6 in. long 3/4 in Nelson headed studs. The shear studs were welded through the steel deck to the beams top chord at approximately the same spacing (12 in.). All welds were tested by "sounding" the studs with a hammer, and questionable studs were given a 15 degree bend test. Faulty studs were replaced and retested. The final design called for a total of 34 studs for both beams. The actual number of studs employed was 38 per beam, allowing for double studs in the two end flutes.

The beam ends were not supported on rollers as for most laboratory tests, as the simulating the influence of weak but realistic end restraints was a part of the program. The end supports for both beams were designed to reproduce the situation where a secondary beam or a main beam is framing into a floor column. Stub columns 6 ft. long were placed into a 3 ft. deep concrete mold and concrete was then cast. After concrete hardened the concrete block with the stubs were bolted to the rigid floor slab. The steel beams were attached to the flanges of steel column stub by means of double clip angles (L 5x5x1/2) allowing for three rows of 3/4 in. A325 LeJeune tension control bolts (Fig. 6).

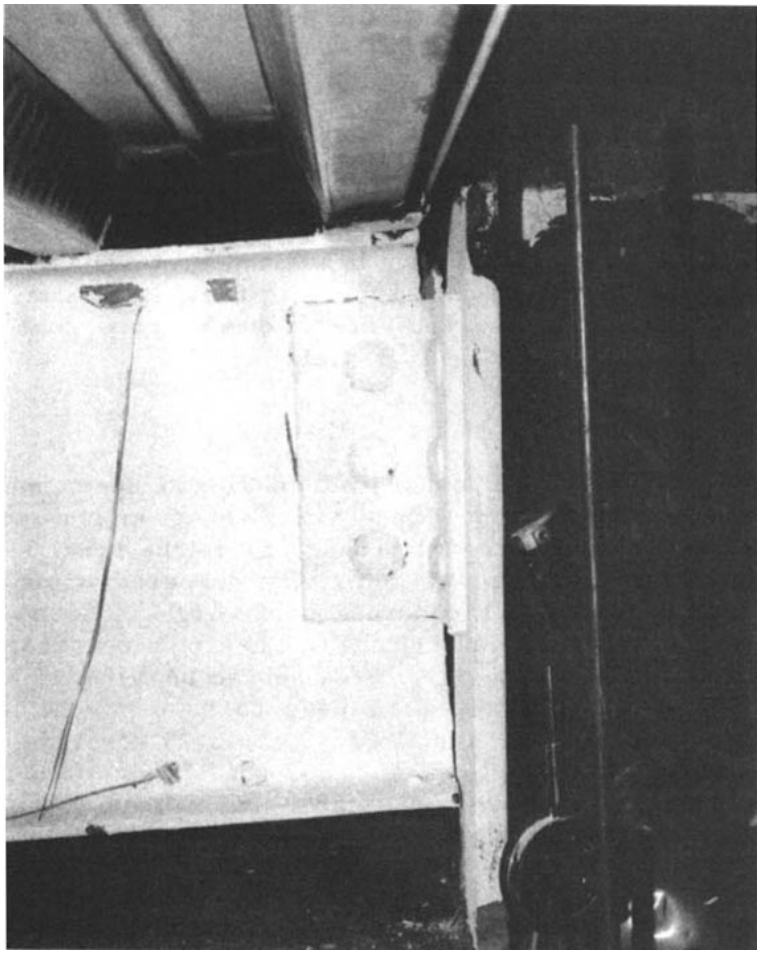

Figure 6 - End supports for test specimens.

The test frame consisted of two 80 K actuators connected to two W12x65 spreader beams 50 in. long. This resulted in a four point load configuration, giving a moment diagram very close to that of a distributed load. The contact between

the loading assembly and the concrete surface was achieved by means of eight 0.5 in. thick 2 x 4 in. steel plates with a 1/2 in. rubber pad under each plate.

Instrumentation

The same instrumentation was used for both specimens. A load cell, and an LVDT attached to each of the hydraulic actuators measured the applied loads and imposed displacements. The actuators were operated on displacement control, using span control in combination with a function generator. The specimens were instrumented with linear variable differential transducers (LVDT's) to measure (1) deflections of top and bottom chords at several points along the span of the beam, (2) end rotations, (3) relative uplift between the steel and the concrete, and (4) slips between the steel joist and the concrete slab. Strain gages were placed on center and quarter points of the span. Dial gages were also used at several locations of the specimen and the loading frame to monitor the course of the test.

Testing Procedure

The testing of both specimens was conducted in the same manner. First an elastic loading cycle was carried out to measure the stiffness of the system, and to insure that all the instrumentation was behaving properly. The total load imposed in the elastic cycles was approximately 50% of the estimated yield load. The second loading sequence was loading until failure. As load was applied, the loads, deflections, rotations and slips were monitored continuously on the data acquisition screen. The test was concluded once the plateau of the load-deflection curve was established and deflection became excessive.

EXPERIMENTAL RESULTS

Beam IV - Shored Construction

Anticipating that the behavior of the composite joist would be essentially elastic up to its estimated yield capacity of 38.3 Kips, an elastic load cycle was carried out to measure the stiffness of the system, and to insure that all the instrumentation was behaving properly. Approximately 33% of the estimated ultimate live load was imposed during this load cycle. No visible cracking of the concrete or evidence of local yielding was noted. The loading was concluded at a total load of 20.0 kips. The total midspan deflection was 0.44 in. from the dead load position for an overall stiffness of 88.0 kips/inch. On unloading from this cycle, the beam responded elastically, with negligible residual deflections.

The second loading cycle was loading to failure. The behavior of the composite beam can best be described by examining Fig. 7, where total test load is plotted versus midspan deflection of the specimen. The composite beam performed elastically up to a load of 35.0 kips, which is very close to its expected yield. At this point the midspan deflection was 0.63 in., which shows a secant stiffness of 56.5 k/in. Small non-linearities gradually increased until a load of 50.0 kips and a corresponding midspan deflection of 1.14 in. was reached. Very limited yielding of the bottom flange of the beam was noticeable at this point.

Shortly after debonding sounds were heard as the metal deck began to separate from the concrete slab at several locations. At a load of 56.8 kips the two

studs on west end of the beam failed, bursting out the surrounding concrete in the form of a cone with a base length of 18 in. After a few small increment of

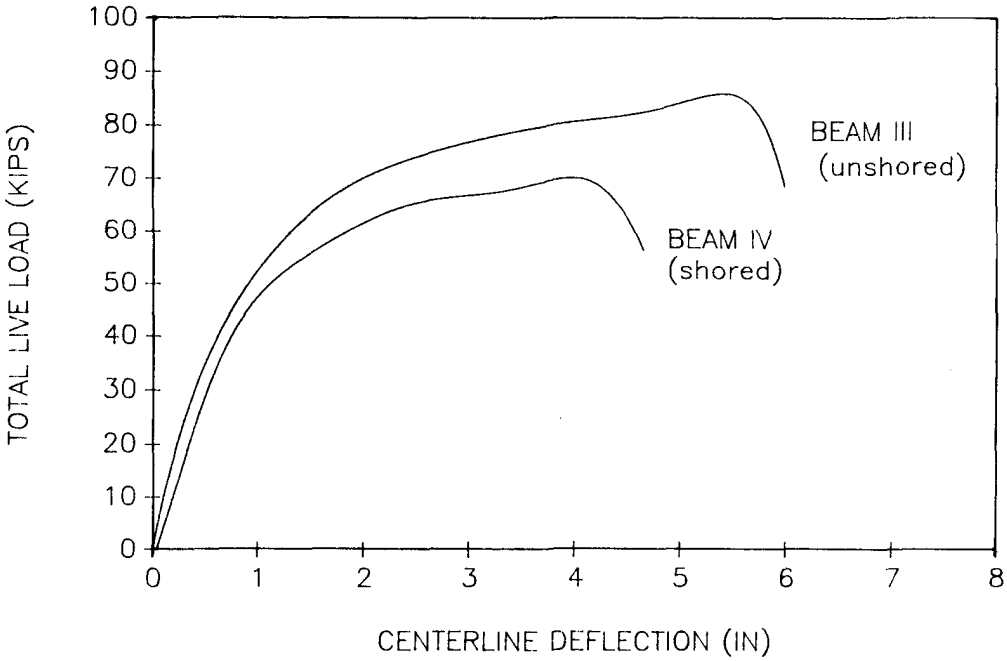

Figure 7 - Load-deflection curves for the entire tests.

load, signs of yielding were observed on the web of the beam at the midspan, and started propagating upwards as load increased. The load-deformation curve started to flatten out reaching higher midspan deflections with no significant increase in load. At a load of 70.5 kips, a corresponding midspan deflection of 4.06 in., and a bottom chord midspan strain of almost 6000 microstrain, the specimen reached its ultimate capacity. This capacity was about 15% over the expected live load ultimate capacity, based on nominal material properties.

Further displacement increments were imposed, and yield lines started propagating rapidly in the midspan section of the steel beam and around the bolt holes at the connection. Shortly after a series of loud bangs announced the sequential failure of the shear studs of the West end and the system capacity dropped down to the capacity of the steel beam alone. The loss of the shear connection made impossible for the specimen to achieve its previous capacity. The beam, however, exhibited considerable ductility before it failed.

Beam III - Unshored Construction

As for the shored beams, an elastic cycle resulted in no visible cracking of the concrete, or local yielding of the steel. The maximum load for this cycle was 15.0 kips and the total midspan deflection was 0.18 in., for a secant stiffness of 85.2 kips/in. On unloading from this cycle, the beam responded elastically, with no residual deflections.

The second loading cycle was loading to failure (Fig. 7). The composite beam elastic performance lasted up to a load of 56.0 kips, demonstrating a longer linear portion of the load-deflection than Beam IV. Midspan deflection at yield was 0.37 in. During the next loading increments debonding noises of the

concrete slab beginning to separate from the metal deck were heard at several locations along the span of the beam. Cracking of the whitewash on the bottom flange of the beam indicated limited yielding. The yield lines started propagating through the web as the loading progressed. At a load of 60.0 kips and a deflection of 1.3 in., the load-deflection curve started to flatten. At this stage a thorough inspection of the specimen did not indicate any damage to the specimen or the connection, or signs of slips or uplift of the deck.

As load was increased yield propagation was evident at midspan and debonding noises became more frequent. The clearance between the beam bottom flanges and the face of the column stubs diminished, indicating the beginning of slip of the bolts. The load-deflection curve reached its peak at a load of 82.0 kips, a centerline deflection of 5.72 in., and a bottom flange centerline strain of about 7200 microstrain. The ultimate capacity of the section was about 30% over the estimated ultimate live moment capacity. Shortly after this stage, just as for Beam IV, the system announced its failure by a pronounced yielding and a series of loud bangs that indicated the failure of studs in the last few flutes of the west end of the beam. The test was terminated at that point, with a midspan deflection was about 8.0 in. (Fig. 8).

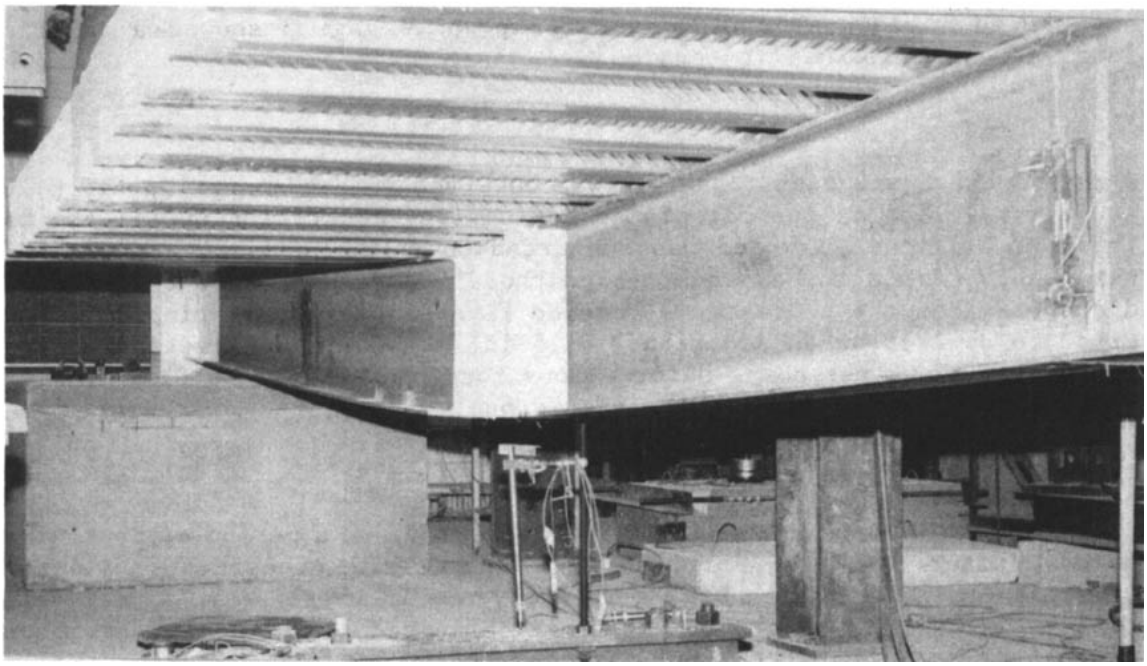

Figure 8 - Beam IV at the end of the test.

INTERPRETATION OF THE RESULTS

The entire load histories for the two beams up to the full design live load are shown in Figure 9. The time scale (horizontal axis) is not uniform in order to render the plot more readable. The initial position was assumed to be a perfectly straight beam with no initial imperfections. Thus for the actual deformations due to full load, applied 80 days after construction, the total deformation at centerline was L/368 for Beam III (unshored) and L/724 for Beam V (shored).

Initial Stresses

Initially Beam III was given a 0.75 in. camber, which was calculated to offset dead load deflection. A calculation of the required camber for simply-supported beam indicated that 1.00 in. would be required; however, because the end restraints were included in the calculation, only 3/4 of this camber was actually applied.

The beam was mechanically cambered with a two point load system, and the strains at the centerline section were monitored. While the residual stresses due to rolling and straightening were not measured, some idea of their magnitude can be inferred from the strains measured during cambering. Figure 10 shows the strains measured near the flange tips of the top and middle of the top flange (gages 5 and 6) and near the tip of the bottom flanges (gages 1 and 3) as the cambering progressed. The data indicates very uneven yielding across the section. For example gage 6 shows yielding at only 800 microstrain of tension, indicating a residual tensile stress after rolling and straightening of about 18 ksi. On the other hand, gage 3 shows yielding near 1800 microstrain, indicating an initial residual compressive stress of 12 ksi. After cambering, gage 6 showed a residual stress near zero, while gage 3 showed a compressive residual stress of 18 ksi in tension.

Casting

When the concrete was cast, Beam III was observed to sag approximately 0.76 in. This was very close to its calculated deflection, and taking up all the camber in the beam. Beam III, which was supported on three jacks with a wooden shim on top, was observed to have compressed those wooden blocks by 0.25 in. as the wood crept. When the shores were removed five days after casting, Beam IV was observed to deflect by an additional 0.15 in. of midspan deflection due to its self-weight. Thus the total deformations for this stage were 0.76 in. for the unshored beam and 0.40 in. for the shored one.

Creep and Shrinkage

The creep and shrinkage deformations were measured for a period of approximately sixty days after casting. For Beam IV (shored), the creep deformations refer only to the time after the shores were removed. In total Beam III deflected by a total of about 0.24 in., while Beam IV deflected by 0.22 in. It should be noted that while the changes in deflection with time were becoming smaller at this stage, they had by no means reached their ultimate values.

The strains on the concrete slab were measured using embedment gages, and showed a significant amount of initial plastic shrinkage even though the specimens were kept wet and covered. For the purposes of discussion the creep and shrinkage strains were zeroed at three days to eliminate these initial effects. Beam III showed an average change of 460 microstrain at the top centerline of the slab, and 450 microstrain at the quarter points after 63 days. For Beam IV, the average at centerline was 190 microstrain, and 390 microstrain at the quarter points. Local measurements of creep and shrinkage vary considerably, of course, but the values reported seem very reasonable when compared to those of other researchers [9,10].

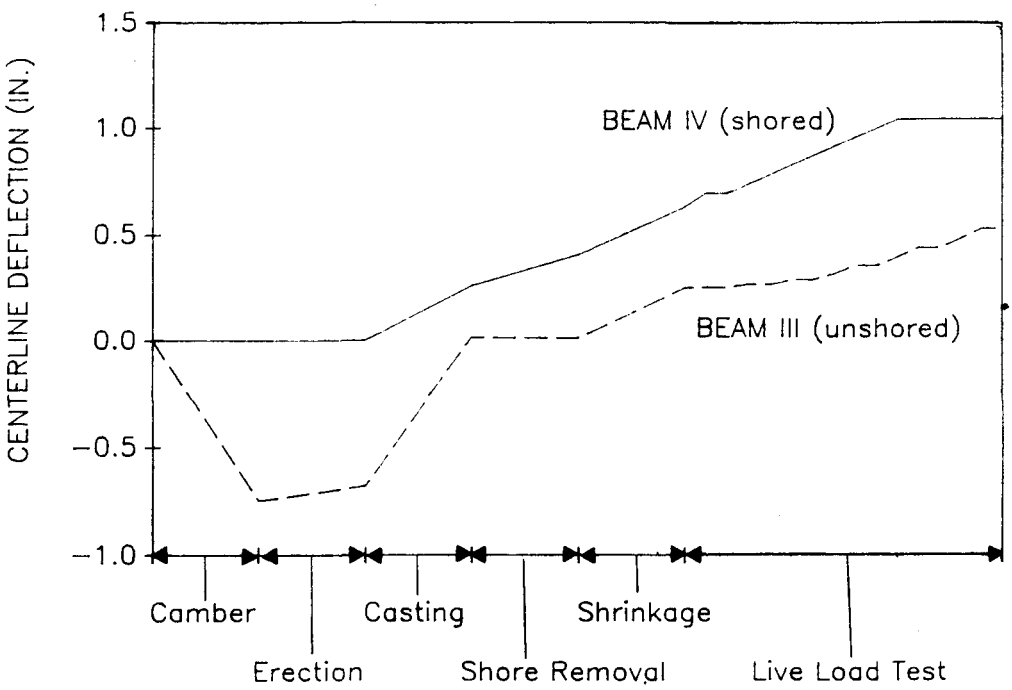

Figure 9 - Entire deflection histories.

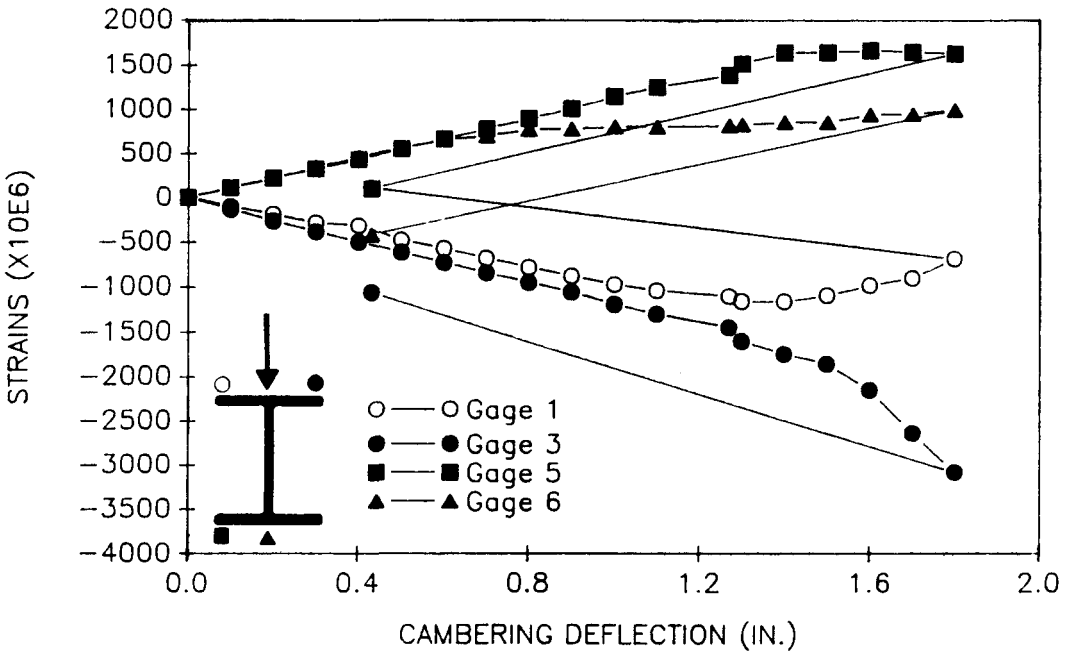

Figure 10 - Stresses measured during cambering.

End Restraint

The degree of end restraint provided by the double angle web connection is difficult to quantify. Although formulas can be found in the literature for initial stiffness and ultimate moment capacity for these connections, the scatter in the data is very large. For Beam III, calculation of the ratio of centerline to end moments during the casting sequence indicate that 76% of the moment went as positive moment at the center and 24% as negative moment to the connection. Recalling that for a fixed-fixed beam the ratio of positive to negative moments is 2:1, the ratio of about 3.2:1 measured implies a large degree of initial end fixity. Similar calculations for Beam IV for the removal of the shores indicates a much smaller amount of end restraint, with the ratio being about 5.0:1.

Behavior under Service Loads

Figure 11 shows the stiffness of the system during live loading. As can be seen, Beam IV showed a slightly larger stiffness initially, although the system stiffness is very similar for both specimens with an offset of about 0.08 in. between the two. The important point to notice is that the stiffnesses decreased consistently, and that by the time L/360 (1.07 in.) is reached the beams are definitely performing non-elastically. The initial stiffness corresponding to a simply-supported beam would have been about 82 kip/in for the elastic moment of inertia (2370 in_4) and 62 kip/in for the lower bound moment of inertia in LRFD (Fig. 12).

Behavior at Ultimate

The ultimate strength of the beam was governed by the shear studs. In the design of the beams nominal values for stud resistance (21.9 kips/stud) and steel yield strength (36 ksi) were used. The 19 studs provided on each side of centerline correspond to 416.1 kips of horizontal shear resistance at the steel-concrete interface. The total A_sF_y without a ϕ factor was 370.8 kips. However, because the actual steel yield strength was 43.3 ksi, the latter number was actually closer to 445.9 kips. Thus the shear studs were weaker and, as described in a previous section, were the source of failure at ultimate. The ultimate capacity of the beam should have been about 83.3 kips (without any ϕ factors), while the failure occurred at a load of 70.5 ksi for Beam IV and 82.0 ksi for Beam III.

The slip began immediately with the application of the first load, and at first appears to have a linear relationship with the applied load. However, in general the linear relationship quickly becomes nonlinear as the amount of slip increased rapidly with small increments of load. The slip was extremely large near the supports, indicating that the end shear connectors are subjected to more shear force than those near the center (Figure 13).

An examination of the slip data clearly shows that both specimens did not behave in a fully composite manner. The relative movement between two adjacent surfaces, as is the case for incomplete interaction, makes it necessary that the use of the elastic theory be modified to take into account the strain discontinuity in evaluating the strength and service characteristics of such members.

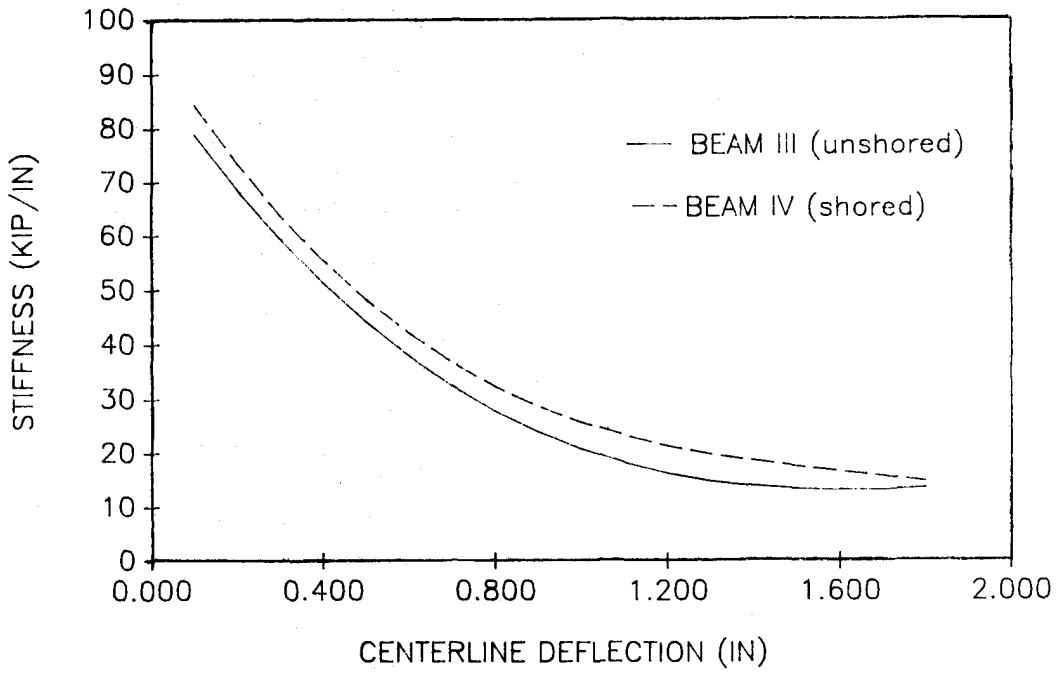

Figure 11 - Changes in stiffness with loading up to 2.00 in. deflection.

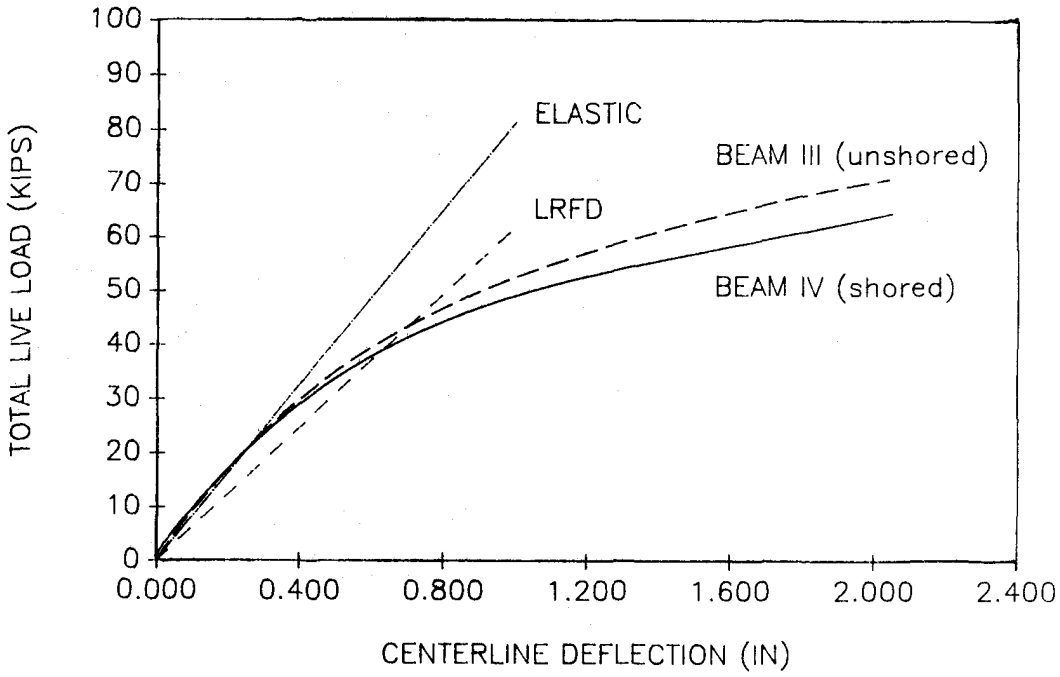

Figure 12 - Measured vs. predicted deflections.

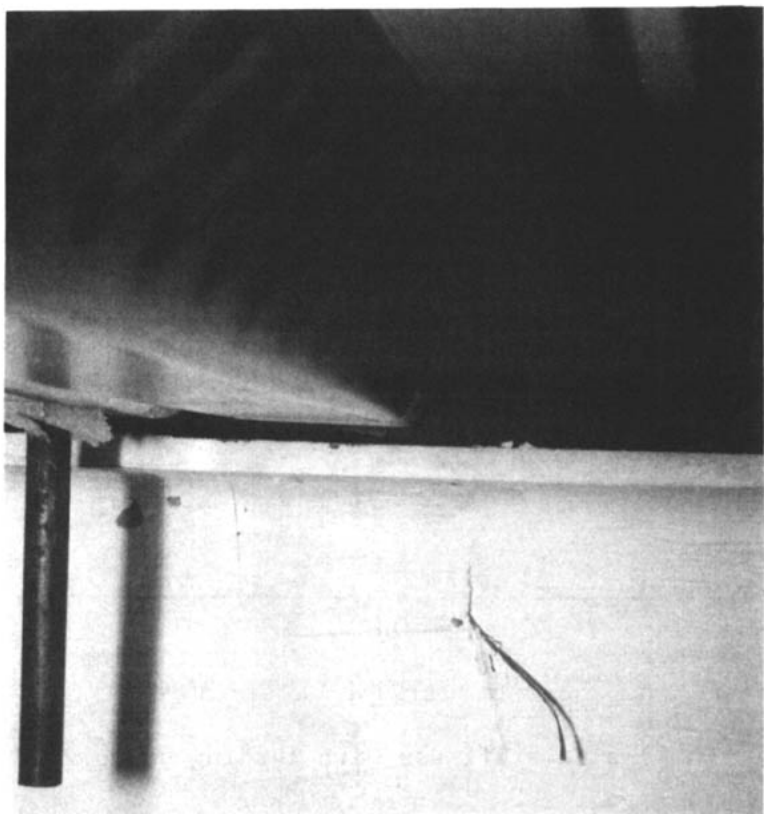

Figure 13 - Separation between deck and beam at end of the test.

CONCLUSIONS

This investigation has shown that:

(1) Long-term deflections, particularly shrinkage, can have a significant effect on composite beam deformations. For long-span, shallow beams (span/depth greater than 20) at least a shrinkage deflection corresponding to 200 microstrain of restrained shrinkage should be incorporated.

(2) Until more exact procedures are proposed and checked, the use of the lower bound moment of inertia suggested in the LRFD specification can be used to calculate the short term deformations due to live loads.

(3) Limited yielding will occur even before the full live load is achieved for most LRFD-designed beams. This is not a major problem if the LBMI is used in the deflection calculations.

(4) The end restraint can have a significant impact on the deflections. Most connections, such as the ones used in these experiments, provide a surprising degree of restraint at low levels of load. It would be very helpful to provide some reinforcing bars across the supports to significantly enhance this capability and extend it into the inelastic range.

REFERENCES

1. Moore, W.P., "Mixed Systems, Past Practice, Recent Experience and Future Direction," in Composite and Mixed Construction (C. Roeder, ed.), Proceedings of the U.S./Japan Joint Seminar, ASCE, New York, 1985, pp. 138-149.

2. Ritchie, J.K., and Chien, E.Y.L., "Construction of Composite Floor Systems in Buildings," in Composite Construction (C. Dale Buckner and Ivan M. Viest, eds.), Proceedings of an Engineering Foundation Conference, ASCE, New York, 1988, pp. 358-373.

3. AISC, "Manual of Steel Construction," 8th Edition, American Institute of Steel Construction, Chicago, 1980.

4. AISC, "Manual of Steel Construction - LRFD," American Institute of Steel Construction, Chicago, 1986.

5. CSA, "CAN3-S16.1-M84 - Steel Structures for Buildings (Limit States Design)," Canadian Standards Association, Rexdale (Toronto), Canada, December, 1984.

6. Vallenilla, C. and Bjorhovde, R., "Effective Width Criteria for Composite Beams," AISC Engineering Journal, Vol. 22, No. 4, 1985, pp. 169-175.

7. Taylor, A.W., "A Study of the Behavior of Simply-Supported Composite Beams," M.S. Thesis, Dept, of Civil Engineering, U. of Washington, Seattle, 1985, 130 pp.

8. Robinson, H., and Narieane, K.S., "Slip and Uplift Effects in Composite Beams," in Composite Construction (C. Dale Buckner and Ivan M. Viest, eds.), Proceedings of an Engineering Foundation Conference, ASCE, New York, 1988, pp. 487-497.

9. Chien, E.Y.L., and Ricthie, J.K., Composite Floor Systems, Canadian Institute of Steel Construction, Willowdale, Ontario, CANADA, 1984, 333 pp.

10. Brattland, A., and Kennedy, D.J.L., "Shrinkage and Flexural Tests of Two Full-Scale Composite Trusses," Structural Engineering Report No. 143, The University of Alberta, Edmonton, Alberta, December, 1986, 264 pp.

11. ACI Committee 209, "Prediction of Creep, Shrinkage and Temperature Effects in Concrete Structures," in SP-27: Designing for the Effects of Creep, Shrinkage, and Temperature in Concrete Structures, American Concrete Institute, Detroit, Michigan, 1971, pp. 51-93.

12. Viest, I., Fountain, R.S., and Singleton, R.C., Composite Construction in Steel and Concrete for Bridges and Buildings, McGraw-Hill, New York, 1958, 176 pp.

13. Bazant, Z.P., "Prediction of Concrete Creep Effects by the Age-Adjusted Modulus Method," J. ACI, Vol. 69, No. 4, April 1972, pp. 212-217.